*Acta Cryst.* (1962). **15**, 794

# The Re-Orientation Caused by Unidirectional Abrasion on Materials of Rocksalt Structure Type

BY P. S. DOBSON AND H. WILMAN

*Applied Physics and Chemistry of Surfaces Laboratory, Chemical Engineering Department, Imperial College, London, S. W. 7, England*

(*Received* 2 *August* 1961 *and in revised form* 18 *October* 1961)

Electron diffraction has been used to study the surface and subsurface structure of unidirectionally abraded polycrystalline LiF, NaF, NaCl, KCl, KBr, MgO and NiO; and also a rocksalt cube face along ⟨100⟩ and ⟨110⟩.

The LiF and NaF developed one-degree ⟨100⟩ 'abrasion texture' and the MgO ⟨111⟩, like the compression texture of the compacted powders (compressed in a die), and this appears to be associated with the low overall density of the compacts used. The NaCl, KCl and KBr all had a backwardly-inclined ⟨110⟩ one-degree orientation with moderately strong azimuthal preference, closely analogous to the rolling texture, which for KCl is found to be ⟨110⟩. The tilt $\delta$ of the ⟨110⟩ axis increased from 16° at the surface to ~ 22° at > 1000 Å depth. The relation to the friction coefficient is indicated. Little or no one-degree orientation is observed on the abraded NaCl cube face; the surface region showed a large rotational displacement about an axis parallel to the surface and normal to the abrasion direction. The abraded NiO showed a backwardly inclined ⟨100⟩ orientation.

These results show that, even in these relatively brittle materials, abrasion involves strong plastic flow and re-orientation to several thousand Å depth.

## 1. Introduction

Although since about 1930 many investigations of the structure of polished surfaces, particularly of metals, were made by electron diffraction, comparatively few have been made on abraded surfaces. The earlier mainly showed that abraded surfaces are heavily fragmented and disoriented, often yielding only electron-diffraction ring patterns, but sometimes showing strong one-degree orientation as for graphite on abraded cast iron (Finch, Quarrell & Wilman, 1935).

The first clear elucidation of the general nature of the lattice re-orientation caused by unidirectional abrasion was provided by Scott & Wilman (1958). In the abrasion of Be, a [001] one-degree orientation was developed, with its axis tilted by an angle $\delta$ away from the outward surface normal, back towards the direction from which the abrasive particles came. Since $\delta \simeq \tan^{-1}\mu$, where $\mu$ is the friction coefficient, it was suggested that this orientation was a compression texture, the (0001) slip planes becoming aligned at right angles to the compressive force, which was the resultant of the normal load and the horizontal force required just to overcome friction and cause sliding. At a few thousand Å below the surface of a Be single crystal abraded on 4/0 emery paper (particle diameter 5 microns) a transition region was observed, where the orientation gradually changed towards that of the undisturbed main crystal, near which a range of orientations was observed corresponding to a rotation of the initial crystal through an angular range of 30° or more about an axis parallel to the surface and normal to the abrasion direction or nearly so (cf. also Evans, Layton & Wilman, 1951; Agarwala & Wilman, 1955).

Porgess & Wilman (1960) found a similar [001] orientation in the surface regions of abraded polycrystalline graphite, but showed further that the tilt $\delta \simeq \tan^{-1}\mu$, even though $\mu$ varied according to the coarseness of the emery. On the fine grades of emery paper, $\mu$ approximated to that ($\sim 0{\cdot}13$) of graphite/graphite sliding contacts, because the emery was largely clogged by the worn-off graphite.

Face-centred-cubic metals, both polycrystalline and single-crystal, also develop on abrasion such a backwardly tilted orientation, of ⟨110⟩ type like the usual compression texture and rolling texture (Goddard, Harker & Wilman, 1962; cf. also Avient, Goddard & Wilman, 1960; and Wilman, 1960). After abrasion on 4/0 emery paper, the metal to a few hundred Å depth showed $\delta$ much less than $\tan^{-1}\mu_{\mathrm{mo.mo}}$, but $\delta$ increased gradually to 30–35° $\simeq \tan^{-1}\mu_{\mathrm{em}}$ at a few thousand Å depth, where $\mu_{\mathrm{mo.mo}}$ is the $\mu$ of metal (+ oxide) contacts, and $\mu_{\mathrm{em}}$ that of emery/metal contacts.

The results described below now show that abrasion of polycrystalline materials of rocksalt-structure type causes a preferred orientation in the surface regions, with axis tilted backward in NaCl, KCl and KBr but of a type ⟨110⟩ which does not correspond to the compression texture (⟨100⟩) but probably to the rolling texture, with a preferred azimuthal range of orientation. No comparable results appear to have been obtained previously on rocksalt-type structures. On the other hand, Germer (1936) found that filing a PbS crystal on a {100} cleavage face along a ⟨010⟩ direction caused a disorientation consisting of a large

range of forward rotation of the lattice about a ⟨010⟩ axis which was parallel to the surface and normal to the abrasion direction; and Raether (1947) obtained a similar result in the corresponding abrasion of a rocksalt cube face. This rotational disorientation corresponds in type to the transition region observed with abraded metal crystals (see above), and this type was also observed on abraded zinc-blende (Evans & Wilman, 1950).

## 2. Experimental

The polycrystalline specimens were formed by compressing the powders of each material at pressures of 75 tons/in.$^2$ (96 for NaCl and MgO) in a steel die 0·5 in. in diameter. The purity of the powders was stated by the suppliers to be: LiF, 98%; NaF, 99·0%; NaCl, 99·5%; KCl, 99·5%; KBr, 99·0%; MgO, 97%; NiO, 98%; and the mean particle diameter after grinding was of the order of 140$\mu$ for NaCl, KCl, KBr and NiO, and less than 5$\mu$ for LiF, NaF and MgO.

The structure of the plane faces of the cylindrical specimens was studied by electron- and X-ray diffraction (Dobson & Wilman, 1961) and it was found that for LiF, NaF, NaCl, KCl and KBr a compression texture with a ⟨100⟩ axis perpendicular to the surface had been developed, whilst MgO developed a ⟨111⟩ compression texture. In the case of NiO the compacted specimens remained fairly powdery and no compression texture was observed.

The specimens were abraded unidirectionally for about 200 cm. on 4/0 and 3/0 emery paper of mean particle diameter 5$\mu$ and 10$\mu$ respectively, manufactured by Messrs. J. Oakey & Sons, Ltd., London; and also some were slid on Whatman's No. 1 filter papers. A load of 500 or 1000 g. was used, and a sliding speed of about 10 cm./sec.

The abraded surfaces were examined at grazing incidence by electron diffraction using a camera length of 47 cm., and electrons accelerated through 60–70 kV.

The specimens were etched so that the structure at various depths below the surface could be examined. The etches used for the alkali halides were a mixture of water and propyl alcohol, and the concentrations of water, and the corresponding etch rates were: LiF, 35%, 40 Å/sec.; NaF, 50%, 120 Å/sec.; NaCl, 5 and 10%, 10 and 250 Å/sec. (single-crystal NaCl cleavage faces 10 and 200 Å/sec.); KCl, 10 and 20%, 100 and 900 Å/sec.; KBr, 5 and 10%, 35 and 350 A/sec. After being etched, the specimens were dehydrated by washing in propyl alcohol, and dried in a desiccator. To etch the MgO, 1% HCl was used (etch rate 100 Å/sec.), and for the NiO 2% HCl (200 Å/sec.). They were then washed in water, followed by propyl alcohol, and dried in a desiccator.

For comparison with the abrasion texture, compacted KCl specimens were rolled between two stainless-steel rollers of 2·5 in. diameter. Although the specimen tended to break-up, some parts of the material rolled into thin strips about 1 cm. square and 0·2 mm. thick. The rolled surfaces were examined by diffraction of Mo $K\alpha$ X-rays at about 10° grazing incidence, the pattern being recorded on a flat film normal to the beam and 4 cm. from the specimen.

## 3. Results

The results described below were obtained on two different compressed specimens of each material, and were repeated several times on each specimen.

1. *The structure of unidirectionally abraded polycrystalline* NaF *and* LiF

The NaF and LiF surfaces, abraded on dry 4/0 emery paper at 500 g. load, showed a closely similar form of structure and are therefore illustrated here only for NaF. The patterns, such as Fig. 1, from the NaF surface immediately after abrasion, showed well-marked one-degree orientation with a ⟨100⟩ axis normal to the surface, but azimuthally random orientation round this axis, since patterns at all azimuths were virtually identical. No appreciable change in the form of the structure was observed on etching down to 7000 Å depth, the surface then exposed yielding patterns still closely similar to Fig. 1.

Since the above orientation is the same as that of the initial compressed specimen surface, abrasion on a face at 40° to the compression axis was also investigated, and this surface also yielded patterns such as Fig. 1, showing clearly that the normal ⟨100⟩ orientation is developed as a result of abrasion, irrespective of the initial orientation.

The NaF surfaces abraded more finely by sliding on filter paper at 1 kg. load, yielded patterns such as Fig. 1, showing a ⟨100⟩ one-degree orientation, but with its axis inclined by about 10° away from the specimen normal, back towards the direction from which the abrasive surface came. Surfaces exposed by etching to about 250 Å depth showed the same structure as that at the surface.

The LiF surfaces abraded on 4/0 emery paper at 500 g. load showed the same form of structure, normal ⟨100⟩ orientation, down to 1000 Å depth, as on the NaF; but the degree of preferred orientation was very small, the patterns showing continuous rings with only noticeable intensification into arcs on the 200 and 400 ring positions near the plane of incidence.

2. *The structure of unidirectionally abraded polycrystalline* NaCl, KCl *and* KBr

The abrasion was on 4/0 or 3/0 emery paper at 1 kg. load for NaCl and KCl, and 500 g. for KBr. Similar results were obtained from all three materials and are typified by Fig. 2 for the NaCl. This shows that a backwardly inclined ⟨110⟩ one-degree orientation was developed in the surface regions, cf. Fig. 9, the tilt $\delta$ being 16° at the immediate surface.

Comparison of Fig. 2 (obtained with the beam $\perp$ to the abrasion direction) with Fig. 9 (tilted), shows

Fig. 1.

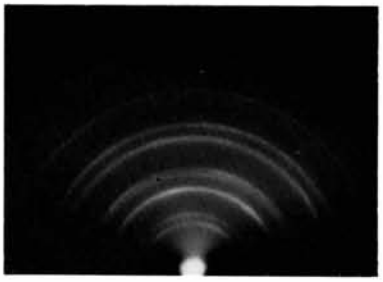

Fig. 2.

Fig. 3.

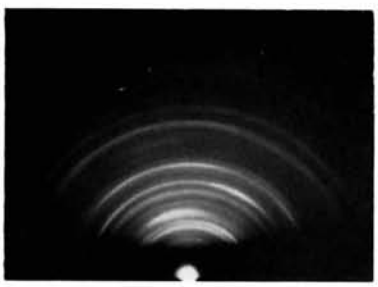

Fig. 4.

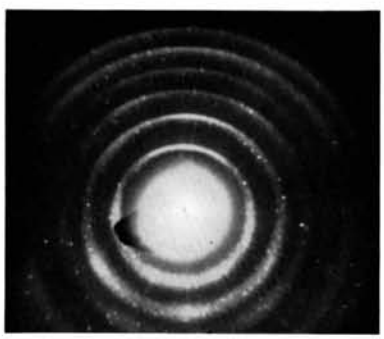

Fig. 5.

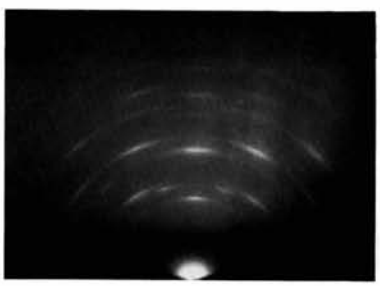

Fig. 6.

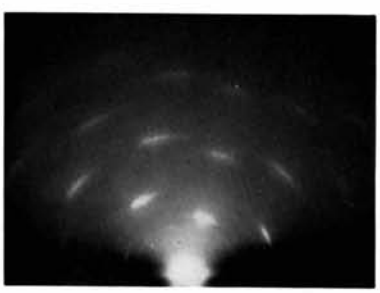

Fig. 7.

Fig. 8.

Fig. 1. Electron diffraction; polycryst. NaF abraded (*L* to *R*) on 4/0 emery; ⊥ r. azimuth. — Fig. 2. As Fig. 1, but NaCl. — Fig. 3. As Fig. 1 but MgO. — Fig. 4. As Fig. 1 but NiO and etched to ~ 1000 Å. — Fig. 5. Rolled KCl, X-ray beam ⊥ r. to *R* direction. — Fig. 6. NaCl (001) face abraded [100] on 4/0 emery; etched 100 Å, beam [100]; electron diffraction. — Fig. 7. As Fig. 6 but etched 3000 Å and beam ⊥ r. to abrasion direction. — Fig. 8. NaCl (001) abrasion [110] on 4/0 emery; etched ~ 200 Å, beam [$1\bar{1}0$].

[*To face p.* 795

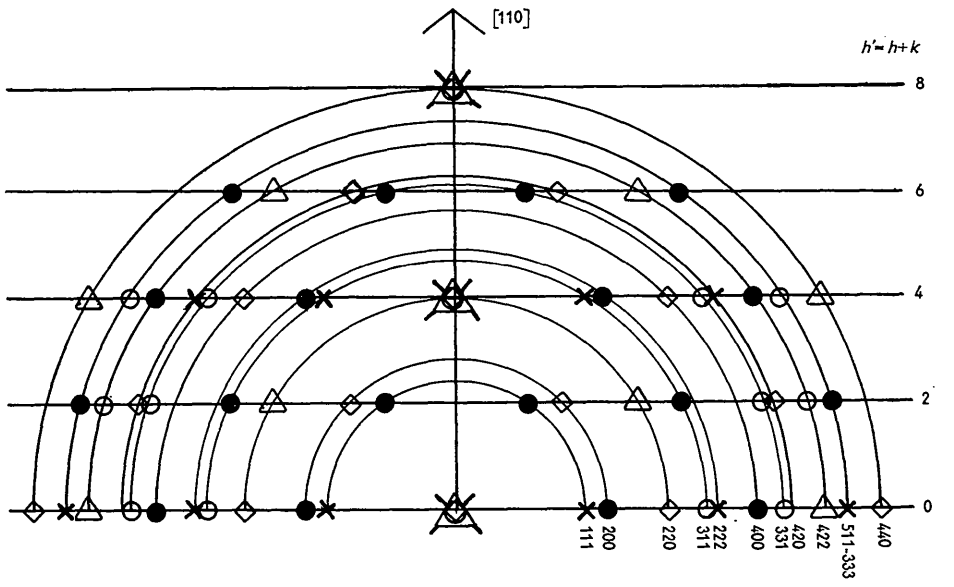


Fig. 9. Diffraction ring positions, and theoretical diffraction positions from a one-degree ⟨110⟩-oriented f.c. cubic structure. Diffractions denoted by ●, △, ×, □, appear when the beam is parallel to directions of type ⟨$\bar{1}$10⟩, ⟨$\bar{1}$11⟩, ⟨$\bar{1}$12⟩ and [001], respectively, while ○ denotes diffractions appearing at the remaining azimuths.

that the strong diffraction arcs correspond to a preferred azimuthal orientation. These strong arcs include (i) the centred-$\sqrt{2}$-rectangle pattern of arcs represented by the filled-in circles in Fig. 9, (ii) the hexagonal arc pattern represented by the triangles in Fig. 9, (iii) the rectangular pattern represented by the crosses in Fig. 9. These patterns correspond to crystals being present in azimuthal orientations such that a direction of ⟨$\bar{1}$10⟩, ⟨$\bar{1}$11⟩, and ⟨$\bar{1}$12⟩ type, respectively, in the {110} plane, is normal to the abrasion direction. The azimuth corresponding to a ⟨001⟩ direction being normal to the abrasion direction, was not, or scarcely, present, because there is negligible intensity (apart from some continuous ring component of the pattern) on the 200 ring at the level for which $h+k=2$ (cf. Fig. 9), although the 111 arcs are strong at this level, as is seen in Fig. 2. The mean preferred azimuthal orientation may therefore be either with a ⟨001⟩ direction along the abrasion direction, or with a direction inclined away from this, such as ⟨$\bar{1}$12⟩, along the abrasion direction. In the first case the spread of orientation from the mean is $>55°$, in the second $>35°$, in azimuth.

Patterns obtained at azimuths about 30°, 60° and 90° from the 'perpendicular setting' showed changes in the relative intensities of the arcs in accordance with these conclusions.

In addition to the above main ⟨110⟩ orientation there was also sometimes a small proportion of the NaCl oriented with a {100} plane parallel to the surface or nearly so. This orientation disappeared when the specimen was etched to about 200 Å depth.

As the NaCl, KCl and KBr specimens were etched, the tilt $\delta$ of the ⟨110⟩ orientation axis increased

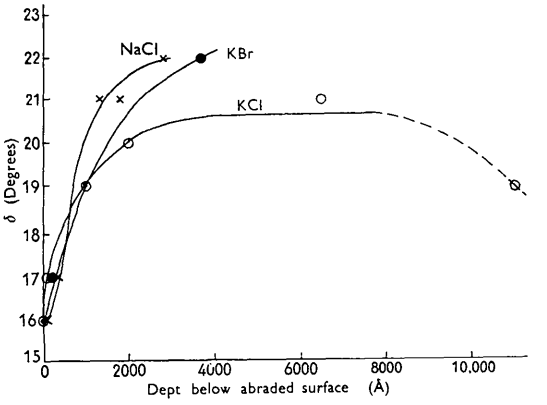


Fig. 10. Variation of tilt $\delta$ of the ⟨110⟩ orientation axis, with depth below the surface of NaCl, KCl and KBr, after abrasion on 4/0 emery paper (at 500 g load for the KBr, and 1 Kg for the NaCl and KCl).

progressively, but more or less flattened off at depths larger than a few thousand Å, as shown in Fig. 10. The abrasion grooves were still visible at depths up to at least 1 micron; and at about 4000 Å depth or more, the electron-diffraction patterns consisted of spotty arcs indicating that the halide was in the form of relatively large crystal blocks.

### 3. *The structure of the unidirectionally abraded polycrystalline* MgO

The surface; after abrasion on 4/0 emery paper at 1 kg. load, yielded patterns such as Fig. 3, with the beam perpendicular to the abrasion direction. This shows a ⟨111⟩ orientation with the axis tilted back

at $\delta \sim 8°$, with no clear indication of any azimuthal preference of orientation round this $\langle 111 \rangle$ axis.

4. *The structure of the unidirectionally abraded* NiO

The immediate surface of the NiO abraded on 4/0 emery paper at 500 g. load yielded patterns which consisted of continuous rings. On etching down to 1000 Å depth, however, patterns such as Fig. 4 were obtained, showing that a $\langle 100 \rangle$ orientation was developed with its axis tilted back at $\delta \sim 16°$; and there was no indication of any marked azimuthal preference of orientation round this axis. Fig. 4 also shows several extra rings which were not observed from the surface before etching, but which might be due to some impurity initially present which was not etched away as rapidly as the NiO.

5. *The structure of unidirectionally abraded* NaCl (001) *cleavage faces*

The abrasion used was on 4/0 emery paper at 500 g. load.

(i) *Abrasion along a* [100] *direction.*—The electron-diffraction photographs from the abraded surface showed only faint arcs superposed on relatively strong continuous rings. Slight etching to about 50 Å depth removed this heavily disoriented surface layer, and after etching to $\sim 100$ Å depth, patterns such as Fig. 6 were obtained in the parallel setting, i.e. with the beam parallel to the abrasion direction. The well-defined arcs in Fig. 6 lie on vertical layer-lines and indicate a range of lattice rotation about the cube edge $\langle 010 \rangle$ which was parallel to the surface and perpendicular to the abrasion direction. In the perpendicular setting the pattern correspondingly consisted of long $hk0$ arcs in a square array, indicating the same rotation axis. The ends of the arcs nearest to the plane of incidence corresponded to a rotational displacement $\delta$ of about 22° from the initial crystal orientation, and the mean of the spread of the arc was at $\delta \sim 40°$, while the arcs extended a further 40–50° beyond this mean, to $\delta \sim 80$–$90°$. An additional arc of moderate intensity was present on the 220 ring position, and may be attributed to some NaCl in backwardly tilted one-degree $\langle 110 \rangle$ orientation being also present, this arc having its centre on a radius at about 60° to this $\langle 110 \rangle$ axis (cf. Fig. 9).

The specimen was etched further to 1000 Å depth and then in stages down to 20,000 Å depth. Again patterns of the above $\langle 010 \rangle$ rotation type were obtained, such as Fig. 7 at a depth of 3000 Å, with now no additional arcs. At 20,000 Å depth the pattern consisted of sharp spots (slightly elongated vartically) in a square array, corresponding to the practically undisturbed single crystal. The variation of the range of rotation (about the $\langle 010 \rangle$ axis) observed, is shown in Fig. 11 as a function of depth below the abraded surface. The most strongly rotated region is in the outermost layer down to $\sim 5000$ Å depth.

(ii) *Abrasion along a* $\langle 110 \rangle$ *direction.*—The patterns showed the presence of a heavily disoriented surface layer less than 50 Å thick, again with a trace of one-degree $\langle 110 \rangle$ orientation such as was found on the abraded polycrystalline specimens. Fig. 8, after etching to $\sim 200$ Å depth, was obtained with the beam normal to the abrasion direction. Fig. 8 shows a well-defined pattern of short arcs in a centred-$\sqrt{2}$-rectangle array (with some superposed ring pattern). This indicates a rotational displacement (and a few degrees range about the mean displacement) of the lattice, away from the initial crystal orientation, by about 20° about the $\langle 1\bar{1}0 \rangle$ direction which was parallel to the surface and normal to the abrasion direction. Patterns obtained with the beam along the abrasion direction, confirmed this direction of the rotation axis with high accuracy, since the diffractions lay on vertical layer lines. At deeper regions the rotational displacement was again progressively smaller, but was still about the same axis; and $\delta$ at various depths was about the same as for the $\langle 100 \rangle$ abrasion, cf. Fig. 11.

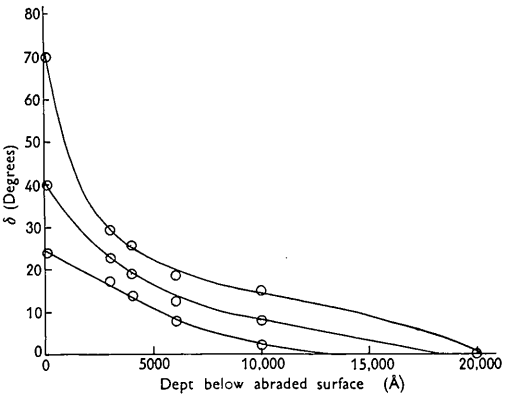


Fig. 11. Mean lattice rotation $\delta$ (middle curve) and the maximum and minimum of the rotation range (upper and lower curves) as a function of depth below the abraded (001) NaCl surface, after abrasion along a cube edge, on dry 4/0 emery paper at 500 g load.

6. *The rolling texture of* KCl

Fig. 5 shows a typical X-ray-diffraction pattern obtained from the rolled KCl strips with the beam at $\sim 10°$ grazing incidence and normal to the rolling direction. The strong 220 and 440 arcs in the plane of incidence show that a $\{110\}$ plane was parallel to the surface or nearly so, in the mean. The arc of 222 type at about the same level as this 220 arc, and the 200 arcs at the level of the central spot show that the azimuthal range of orientation included that having a $\langle 001 \rangle$ direction along the abrasion direction. In the part of the pattern below the shadow edge it is clear that strong arcs of 220 type also occur on radii at about $\pm 60°$ from the plane of incidence; thus the azimuths with a $\langle 1\bar{1}1 \rangle$ type of direction along the beam, i.e. a $\langle 1\bar{1}2 \rangle$ direction along the rolling direction, are strongly represented. Probably the rolling direction

is tending to be along the $\langle 1\bar{1}2\rangle$ type of direction, but with a spread of more than $\pm 36°$ from the mean occurring in the specimen, within the $\sim$ 1 mm. $\times$ 5 mm. region grazed by the beam.

Most of the photographs obtained, such as Fig. 5, also evidently contain weaker diffraction arcs, particularly 200 and 400 centred on the plane of incidence which indicate presence of a moderate proportion of $\langle 100\rangle$ oriented KCl lattice. This component orientation is of the same type as that of the specimens of compacted KCl powder.

## 4. Discussion

Abrasion of these rocksalt-type materials causes grooves of much the same nature as are developed on metals by abrasion, and the present results show similarly that much deformation by plastic flow is involved, i.e. by slip processes, though part of the groove volume is removed as wear debris, at least in some grooves where favourably shaped and oriented abrasive particles exert a cutting action (cf. Avient, Goddard & Wilman, 1960).

### 1. *The orientation on the abraded polycrystalline salts of* NaCl *type, in relation to the compression and rolling textures*

Whenever the surface regions of the abraded polycrystalline materials showed an orientation having no azimuthal preference, the type of orientation corresponded to the compression texture, that was observed in the initial diecompacted material, i.e. $\langle 100\rangle$ for NaF and LiF, and $\langle 111\rangle$ for MgO (Dobson & Wilman, 1961).

Though the compression texture observed in NaCl, KCl and KBr compacted in a die was also $\langle 100\rangle$ (Dobson & Wilman, 1961), these showed mainly a backwardly inclined $\langle 110\rangle$ orientation (azimuthally moderately strongly limited) on the abraded surfaces, with only a trace of $\langle 100\rangle$ orientation also present in the case of the NaCl, this being evidently also caused by the abrasion, since it was removed by a slight etching.

This azimuthally limited $\langle 110\rangle$ type of orientation is of the same type as the $\langle 110\rangle$ rolling texture which was determined for the KCl (see § 3·6). It was also observed (King & Wilman, 1961; King, 1960) on unidirectionally abraded AgCl and AgBr, with similar azimuthal preference; and it was shown to correspond to the $\{110\}\langle 1\bar{1}2\rangle$ rolling texture of these silver halides (King & Wilman, 1961). It is therefore indicated that the NaCl, KCl and KBr, like the AgCl and AgBr, are relatively highly deformable by slip during abrasion, in spite of the marked cleavability of these alkali halides. The plastic flow and re-orientation are evidently closely analogous to those occurring in rolling, as was concluded for the cases of unidirectionally abraded or scraped Zn, Cd, and the f.c. and b.c. cubic metals (Goddard, Harker & Wilman, 1961). Although the texture developed in AgCl and AgBr when the granular material was compressed in a die was $\langle 100\rangle$ with some slightly oblique $\langle 111\rangle$, that developed when the halide was compressed between lubricated polished stainless steel plates was $\langle 110\rangle$; this evidently corresponding to extensive lateral (radial) flow, nearly equivalent to rolling radially. In the present case of abrasion, the compression is indeed under conditions permitting extensive lateral flow round the indenting tips of the abrasive particles, and a tilted $\langle 110\rangle$ orientation is observed, although there is azimuthal preference, as for rolling. The plastic flow appears therefore to be of a type having close analogies to both rolling and compression.

### 2. *The angle of inclination $\delta$ of the orientation axis*

It is noteworthy that in the LiF, NaF and MgO the surfaces showed prominent orientation but with only small $\delta \simeq 0$–$8°$. This small $\delta$, together with the fact that the orientation agrees in type with the compression texture, appears to show that the plastic flow in these materials was mainly caused by the vertical load, whilst there is little or no plastic deformation resulting from the forward motion of the abrasive particles. In these materials the particle size was small, $<5$ microns, and also the specimens were compacted to only about 60% of the true density, i.e. the volume of the voids is comparable with that of the particles. The relative motion of the contacting regions during sliding on the emery is thus likely to lead to some grains being broken off and pushed into neighbouring voids; and this will reduce the effect of the forward motion, additional to the plastic flow by simple loading. The fact that rocksalt-type crystals are plastically deformable in compression, but essentially brittle in tension, may also be involved.

The variation of $\delta$ with depth below the surface of the abraded NaCl, KCl and KBr, shown in Fig. 10 is similar for all these materials, and $\delta$ became almost constant at depths greater than 1000 Å.

It is of interest to compare $\delta$ with the inclination ($\tan^{-1}\mu$) of the resultant of the normal load and the tangential force required to overcome friction. The coefficient of friction, $\mu$, on the 4/0 emery paper under the above conditions, was found to be 0·44, 0·49, and 0·47, for the NaCl, KCl and KBr respectively. The $\mu$ for the NaCl (0·44) was slightly larger than the $\mu$ (0·28) of NaCl sliding on NaCl, and indeed this corresponds to most of the load being supported on NaCl contacts with the worn-off NaCl which largely clogs the fine emery paper. The $\delta \sim 16°$, observed at the abraded surface, thus agrees well with $\tan^{-1}\mu_{\mathrm{NaCl/NaCl}}$. At lower regions $\delta$ is larger and becomes nearly constant at $>1000$ Å depth, and this value $\sim 22°$ agrees well with $\tan^{-1}\mu$, i.e. $\tan^{-1}(0{\cdot}4)$ for the specimen sliding on 4/0 emery. It is less than $\tan^{-1}\mu_{\mathrm{e/NaCl}}$, where $\mu_{\mathrm{e/NaCl}}$ is the coefficient of friction to the NaCl on emery in absence of clogging, which

is observed to be 0·78 on emery papers of particle diameter larger than about 50 microns.

3. *The structure of unidirectionally abraded* NaCl *crystal cleavage faces*

Although electron-diffraction investigations of the surface structure of these single-crystal faces abraded on 4/0 emery paper (along a cube edge and a cube-face diagonal respectively) were made at the surface and after various stages of etching, only traces of one-degree orientation were observed in the uppermost ~100 Å thick region. On the other hand, after etching to ~50 Å depth, the randomly disoriented surface region was removed, and the patterns then showed that plastic flow had mainly resulted in a large range of lattice rotation from the initial single crystal, about an axis parallel to the surface and normal to the abrasion direction. This surface orientation is of the type observed by Germer (1936) on a filed galena cube face, and by Raether (1947) on an abraded NaCl cube face. It is typical of the lower transition region to the undisturbed substrate, such as was found in the case of abraded metal crystals (cf. Evans, Layton & Wilman, 1951; Agarwala & Wilman, 1955; Scott & Wilman, 1958; Goddard, Harker & Wilman, 1961). It was concluded (Scott & Wilman, 1958) that these regions probably undergo some rotational slip which then allows flexure of the slip lamellae about an axis in their plane and normal to the abrasion direction (flexural rotational slip). In both the above cases of NaCl the axis of rotation observed could correspond to flexural translational slip on $\{110\}$ along $\langle 1\bar{1}0\rangle$, since the axis of rotation observed was parallel to this slip plane and normal to this slip direction.

Our measurements of the friction coefficient $\mu$ and the wear/cm. $M$ of the NaCl specimens, as a function of the particle diameter $D$ of the abrasive, will be described elsewhere. The $\mu/D$, $M/D$, and $M/\mu$ relationships observed for the single-crystal cube face were very closely similar to those found for the polycrystalline specimens, notwithstanding the absence of any one-degree $\langle 110\rangle$ oriented surface region.

The above work was carried out with the financial support of the Atomic Power Division of The English Electric Company Ltd., and we thank Mr H. H. Heath for kindly arranging for the preparation of most of the compacted specimens. We also thank Dr G. S. Parry of the Chemical Engineering Department, Imperial College, for the use of the X-ray diffraction apparatus.

## References

AGARWALA, R. P. & WILMAN, H. (1955). *J. Iron Steel Inst.* **179**, 124.

AVIENT, B. W. E., GODDARD, J. & WILMAN, H. (1960). *Proc. Roy. Soc.* A, **258**, 159.

DOBSON, P. S. & WILMAN, H. (1961). *Acta Cryst.* **14**, 1275.

EVANS, D. M., LAYTON, D. N. & WILMAN, H. (1951). *Proc. Roy. Soc.* A, **205**, 17.

EVANS, D. M. & WILMAN, H. (1950). *Proc. Phys. Soc.* A, **63**, 298.

FINCH, G. I., QUARRELL, A. G. & WILMAN, H. (1935). *Trans. Faraday Soc.* **31**, 1030.

GERMER, L. H. (1936). *Phys. Rev.* **50**, 659.

GODDARD, J., HARKER, H. J. & WILMAN, H. (1962). In course of publication.

KING, J. N. (1960). M. Sc. Thesis, Univ. of London.

KING, J. N. & WILMAN, H. (1961). *Proc. Phys. Soc.* In course of publication.

PORGESS, P. V. K. & WILMAN, H. (1960). *Proc. Phys. Soc.* **76**, 513.

RAETHER, H. (1947). *Métaux et Corros.* **22**, 2.

SCOTT, V. D. & WILMAN, H. (1958). *Proc. Roy. Soc.* A, **247**, 353.

WILMAN, H. (1960). *Acta Cryst.* **13**, 1062.